

# Investigation of Tonal Noise in a High Pressure Turbine Stage Due to Temperature Inhomogeneous of the Inflow

Mu Zhongqiang<sup>1</sup>, Qiao Weiyang<sup>1</sup> & Ulf Michel<sup>2</sup>

<sup>1</sup> School of Power and Energy, Northwestern Polytechnical University, Xi'an, China

<sup>2</sup> German Aerospace Center, Berlin, Germany

Correspondence: Mu Zhongqiang, School of Power and Energy, Northwestern Polytechnical University, YouYi West road 127#, Xi'an 710072, China. Tel: 86-150-2918-9537. E-mail: xiaoqiang\_npu@yahoo.com.cn

Received: April 27, 2012

Accepted: May 15, 2012

Online Published: May 28, 2012

doi:10.5539/mas.v6n6p64

URL: <http://dx.doi.org/10.5539/mas.v6n6p64>

## Abstract

The tonal sound emission of a high pressure turbine stage due to total temperature inhomogeneous of the inflow investigated numerically. A non-uniform mean temperature made by a result of the discrete burners inside the annular combustion chamber. In present paper we made a setting that 14 periodic total temperature distribution in the azimuthal direction in the turbine inlet. Through comparison between non-uniform inlet temperature case and uniform inlet temperature case, the results show that the sound power emitted in the downstream direction is increased by 5.9 dB at the blade-passing frequency and by remarkably 11.6 dB at the first harmonic of the blade-passing frequency. This result indicated the total temperature fluctuation in the inlet of turbine stage would affect the sound field drastically.

**Keywords:** non-uniform temperature inlet, periodic total temperature-rotor interaction, blade passing frequency, sound pressure level, sound power level

## 1. Introduction

The success in reducing jet noise and fan noise result in core noise becoming relatively more and more important in modern engine. As well known, Part of the core noise is caused by combustion courses. Combustors contribute substantially to the tonal noise that is emitted from the core nozzle of a turbofan engine. This contribution can be separated into direct and indirect combustion noise. Indirect combustion noise is generated in the nozzle guide vanes at the exits of combustors and in the following turbine stages as a result of the unsteadiness of the fluid temperature (Cumpsty & Marble, 1977; 1979).

In recent years, some scientists have done some studies on indirect combustion noise. J. Miles et al. (2010) has developed an experiment method to identify the indirect combustion noise and direct combustion noise into different frequency domain using aligned and unaligned coherence techniques. Bake et al. (2007; 2008; 2009) has also demonstrated the indirect combustion noise by using a electrically heated flow as a inlet flow for a convergent-divergent nozzle tube. A numerical simulation of this simple experimental setup was performed by Leykoa et al. (2009).

A numerical simulation of the indirect combustion noise is much more complicated for a real blade account turbine stage. The computation demanded a huge computation source because of the time-dependent problem. One important simplification is concentrated on the tonal noise emission. Van Zante et al. (2009) concluded that the contribution of temperature fluctuation to overall sound pressure field rather small compared with the viscous and potential field interaction mechanisms by changing the flow rate of the cooling flow to control the temperature fluctuation in the wake flow of the stator vanes. Z. Mu et al. (2010) through setting a periodic total temperature distribution in 2 stator vanes to divide the circumferential mode into rotor-stator interaction mode and periodic total temperature-rotor interaction mode successfully. This method confirmed the indirect combustion noise in a turbine stage, but the difference of sound power level between the non-uniform temperature inlet and uniform temperature inlet was also small.

The temperature distribution in the inflow of a turbine has a steady and an unsteady component. The steady component is caused by the regular array of separate burners placed in the annular combustion chamber, which is typical for an aero-engine, resulting in a periodicity of the mean total temperature in the azimuthal direction.

This steady distribution is overlaid by a random unsteady component. The steady component may generate tones, while the unsteady component gives rise to tonal as well as broadband noise. The objective of this investigation is to estimate the tonal noise emission due to the unsteady temperature distribution by simulation numerically the tonal sound emission and by comparing a reference cases with uniform inflow with a case where the inflow has a periodic variation of the total temperature in azimuthal direction.

From the view of Figure 1, the unsteady disturbances are of the same order of magnitude as the steady parts in the high pressure turbine (HPT) zone which needs to be described by Compressible Navier-Stokes equations, but in the straight duct zone, the unsteady components are small compared to the steady (mean) flow which will be described by Lined Euler Equations. To couple these 2 zones, we use the Triple-plane pressure (TPP) Matching method which developed by Ovenden and Rinstra (2004). Because the disturbances would not affect the processing of sound propagation, in order to simple the problem, we assumed there was no swirling flow in the straight duct zone, which means we get the sound source information using computational fluid dynamics (CFD) method, and sound propagating in a non-swirling flow straight duct zone using computational aero-acoustics (CAA) method. This assumption will be a little non-physical, but will not affect our comparison of present paper.

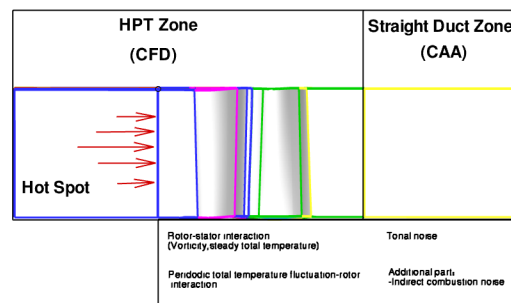


Figure 1. Zones in a typical high pressure turbine stage for the study of tonal noise due to inhomogeneous temperature of inflow

## 2. Method

### 2.1 Turbine and Mesh Topology

The turbine stage consists of 70 vanes and a downstream rotor with 73 blades. There is no tip clearance between the rotor blades and the casing as well as between the stator vanes and the hub, which means that the casing rotates together with the rotor and the hub is stationary at the location of the stator. In addition the outer casing and the inner hub have constant radii. In order to simulate the influence of a stationary temperature distribution, which is periodic in the circumferential direction, it is assumed that the temperature field consists of 14 periodic. Each periodic have 5 stator vanes. The baseline case uses 1 stator passage and 1 rotor passage because of the uniform total temperature of the inflow.

To decrease the effects of acoustic reflection from upstream and downstream boundaries, buffer zones were added to the inlet and outlet duct with a stretching ration of 1:1.2. It can be seen from Figure 2, that the inlet flow is divided into 35 blocks to enable a variation of the total temperature in the azimuthal direction. Figure 2 also shows the rotational part, which is turbine rotor part, and non-rotation part, which including the stator part and two buffer zone part. A view on the grid in the mid-span cylinder is shown in Figure 3. The distance of the first grid point from the surfaces in terms of wall units is generally  $y^+$  plus smaller than 1 at blade surfaces and  $y^+$  plus smaller than 4 on hub and casing.

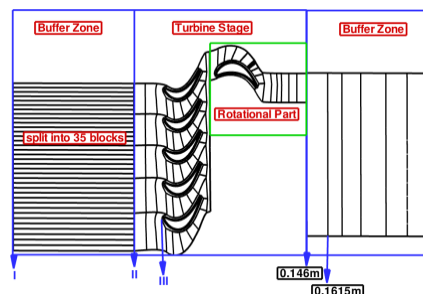


Figure 2. Computation domain

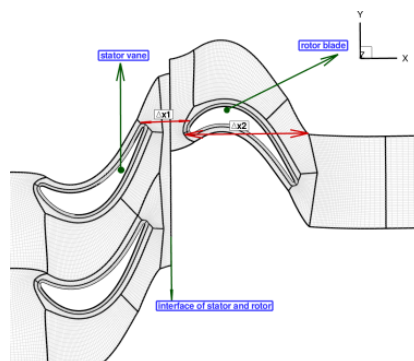


Figure 3. Part of Computation grid

### 2.2 Flow Solver and Grid Limitation

The numerical simulation are performed using the non-linear, compressible three dimensional, Unsteady Reynolds Average Navier-Stokes (URANS) flow solver Turbo-machinery Research Aerodynamics Computational Environment (TRACE) which was developed by the Germany Aerospace Center to investigate turbo-machinery aerodynamics and related phenomena. TRACE allows several parameters to be selected. The  $k-\omega$  model is used here for turbulence closure. The Giles method applied as low-reflection boundary condition in the inlet and outlet boundaries. The Crank-Nicolson scheme was used for time integration. 640 time steps are used per rotor passage and temperature period with 30 sub-iterations each.

The use of phase-lag method which developed by He (1992) is activated in TRACE. This allows to restrict the computational domain to only one period of the temperature field (5 stator passages) and 1 rotor passage. By using this approach the flow in the stationary frame is described by a Fourier series with  $N$  harmonics of the blade-passing frequency  $f_b = B \times f_s = 10220$  HZ, where  $B = 73$  is the number of rotor blades and  $f_s$  is the shaft speed of the rotor. The flow of this investigation is described with harmonic number  $N = 66$  (of the theoretically 128, default value 14 for 1 stator passage and 1 rotor passage) Fourier components.

TRACE requires about 40 grid points per wave length in the wave-normal direction to keep the influences of dissipation and dispersion on the simulation of sound propagation sufficiently small, which means to values of less than 1 dB per wave length (Kaplan et al., 2006). There are 50 nodes between stator vanes and rotor blades ( $\Delta x_1$ ), 80 nodes along the blade chord ( $\Delta x_2$ ). For this case, the grid spacing is fine enough for the blade passing frequency and its first harmonic.

To remove the influence of the spurious reflections and to investigate the sound field downstream of the rotor, the TPP Mode Matching Strategy is used. The three coupling planes  $x = 0.150$  m,  $x = 0.155$  m,  $x = 0.160$  m are chosen here. The results of the mode analyses are described in the plane  $x = 0.155$  m.

### 2.3 Inlet Total Temperature Setting

In the inlet boundary, the total pressure, total temperature, and inlet flow angle are prescribed. The version of TRACE used for this investigation does not allow prescribing a variation of the mean temperature in the azimuthal direction. A workaround for the consideration of a non-uniform inlet temperature distribution is to divide one periodic of the inflow domain into blocks in the azimuthal direction. This is the reason why the domain upstream of the stator was divided into 35 radial slices.

For the uniform temperature inlet case, the total temperature of the inflow is 1100 K. For the non-uniform case, the center of total temperature is 1200 K in each periodic, closing to the hub and casing is about 1000 K. This inlet total temperature setting is more realistic. The flow upstream of the second turbine stage investigated here contains a large swirl resulting from the first stage. In order to achieve a temperature distribution in front of the stator that more or less only depends on the azimuthal position, the temperature distribution at the inlet boundary has to be chosen as soon in Figure 4(a). The azimuthal distribution of total temperature in the inlet of stator is shown in Figure 4(b). The comparison of mass flow-weighted average of total temperature between uniform temperature case and non-uniform temperature case in 3 planes with different axial position is shown in Table 1, and the difference is very small that we can chose the uniform temperature case as the baseline case.

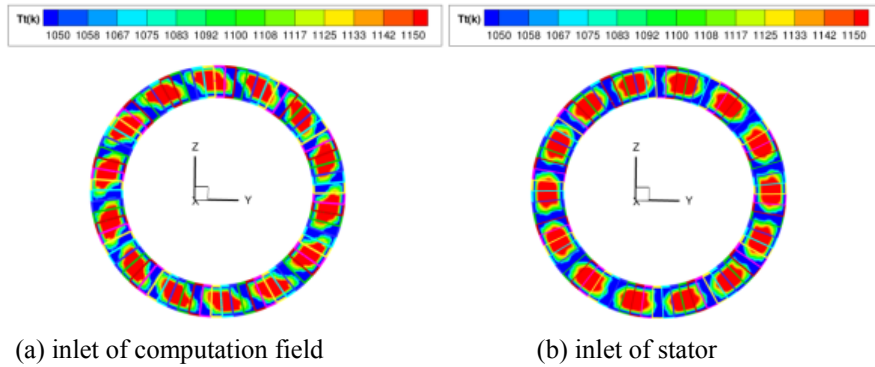


Figure 4. Azimuthal distribution of total temperature

Table 1. Comparison of total temperature in different axial plane

	Mass Flow-weighted Average of total temperature	
	Uniform temperature case	Non-uniform temperature case
I	1100K	1098.199K
II	1100K	1098.652K
III	1100K	1098.674K

2.4 Test Case Description

The test facility designed by the Institute of Propulsion Technology of Germany Space Center in Berlin is composed of 38 outlet guide vane (OGV) and 22 fan blades. All the acoustic modes in fb were cut-off, Dominant cut-on circumferential mode was  $m=6$  in 2fb and  $m=-10$  in 3fb.

Working point of experiment test (Ex) and numerical simulation (Si) is shown in Table 2,  $\dot{m}$  is mass flow,  $\Pi$  is fan pressure ratio, RPM is revolutions per minute,  $p_0$  and  $T_0$  is the total pressure and total temperature, zero means inlet of fan stage. The difference of Sound Pressure Level (SPL) in  $m=6$  between experiment and simulation is 1 or 2 dB (Figure 5(a)); the comparison is not so satisfactory in  $m=-10$  (Figure 5(b)), but the trend of simulation and experiment are same, compared to  $m=6$ , the SPL of both results reduced more than 20 dB. Further details concerning the fan rig can also be found in Kaplan et al. (2006) and Tapken et al. (2009).

Table 2. Working point of experiment and simulation

	$\dot{m}$	$\Pi$	RPM	$p_0 (Pa)$	$T_0 (K)$
Ex	0.489	0.720	3142	100440	289.65
Si	0.461	0.726	3187	101325	288.15

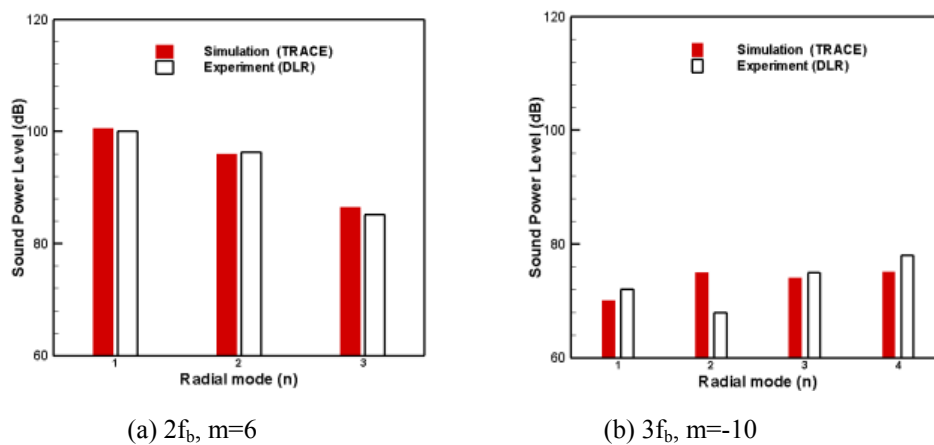


Figure 5. Comparison of SPL on each radial mode for dominant circumferential mode

### 2.5 Mode Analysis

According to the theory of Tyler and Sofrin (1962), the circumferential mode due to rotor-stator interaction is given by  $m = hB - sV$ , here  $m$  is circumferential mode order,  $h$  is multiple of blade passing frequency,  $s$  is running index in Tyler-Sofrin relation,  $B$  and  $V$  is the rotor blade number and stator vane number respectively.

The circumferential mode due to periodic total temperature-rotor interaction is obtained:  $m = hB - sP_T$ , here  $P_T$  is number of azimuthal periods of total temperature on inlet boundary.

Some circumferential mode ( $|m| < 100$ ) produced by rotor-stator interaction or periodic total temperature-rotor interaction is shown in Table 3. For uniform temperature inlet case, circumferential modes just produced by rotor-stator interaction; for non-uniform temperature inlet case, some circumferential just produced by periodic total temperature-rotor interaction, such as  $m = -25, -11, -8$  etc., and other circumferential modes produced by periodic total temperature-rotor interaction and rotor-stator interaction, such as  $m = 3, 6$ , etc.

Table 3. Circumferential mode analysis, number of rotor blades  $B=73$ , number of stator vanes  $V=70$ , number of temperature periods  $P_T=14$

frequency	Rotor-stator interaction		Rotor-temperature interaction		
	s	$m=hB+sV$	s	$m=hB+sP_T$	
h=1 $f_b$	-2	-67(cut-off)	-10	67(cut-off)	
			-9	-53(cut-off)	
			-8	-39(cut-off)	
			-7	-25	
			-6	-11	
			-5	3	
	-1	3	-4	17	
			-3	31	
			-2	45(cut-off)	
			-1	59(cut-off)	
			0	73(cut-off)	
	h=2 $2f_b$	-3	-64	-16	-78(cut-off)
				-15	-64
-14				-50	
-13				-36	
-2		6	-12	-22	
			-11	-8	
			-10	6	
			-9	20	
			-8	34	
			-7	48	
-1	76(cut-off)	-6	62		
		-5	76(cut off)		

## 3. Results

### 3.2 Fluctuation Pressure Analysis in Frequency Field

Figure 6 shows 3-D distribution of fluctuation pressure in the duct of downstream rotor for  $f_b$  and  $2f_b$ . There is no new sound source in this area (assuming no swirling flow exist), and the unsteady aerodynamic became weak

because of the vortex mixture and dissipation. The circumferential mode due to the effect of rotor-stator interaction and periodic total temperature-rotor interaction is obviously, and the amplitude of fluctuation pressure is bigger in non-uniform temperature inlet case.

The fluctuation pressure of downstream of the rotor is plotted in Figure 7 (a) (b) for the blade-passing frequency as function of the circumferential position in the mid-span position for the uniform temperature inlet case and non-uniform temperature inlet case. The circumferential mode number  $m=3$  (see Table 3) can be identified as dominating contribution, since there are three-periods over an angle of  $2\pi$ . The additional mode  $m=-67$  for the non-uniform temperature inlet is clearly visible in Figure 7 (b). Because the number of peaks per  $2\pi$  is 67, the  $m=-67$  affected by the rotor-stator interaction and periodic total temperature-rotor interaction, but this mode was cut-off. The additional mode  $m=73$  (cut-off) for the uniform temperature inlet case is also clearly visible in Figure 7(a).

The fluctuation pressure is shown in Figure 7(c) (d) for  $f=2f_b$ . This frequency is dominated by  $m=6$ . The additional oscillations due to a non-uniform temperature distribution in Figure 7(d) are dominated by the mode  $m=62$ . For the uniform temperature case, the affecting of  $m=-78$  (cut-off) is also visible in Figure 7(c). It can be seen clearly that the pressure field of both frequencies is influenced by the non-uniform temperature distribution.

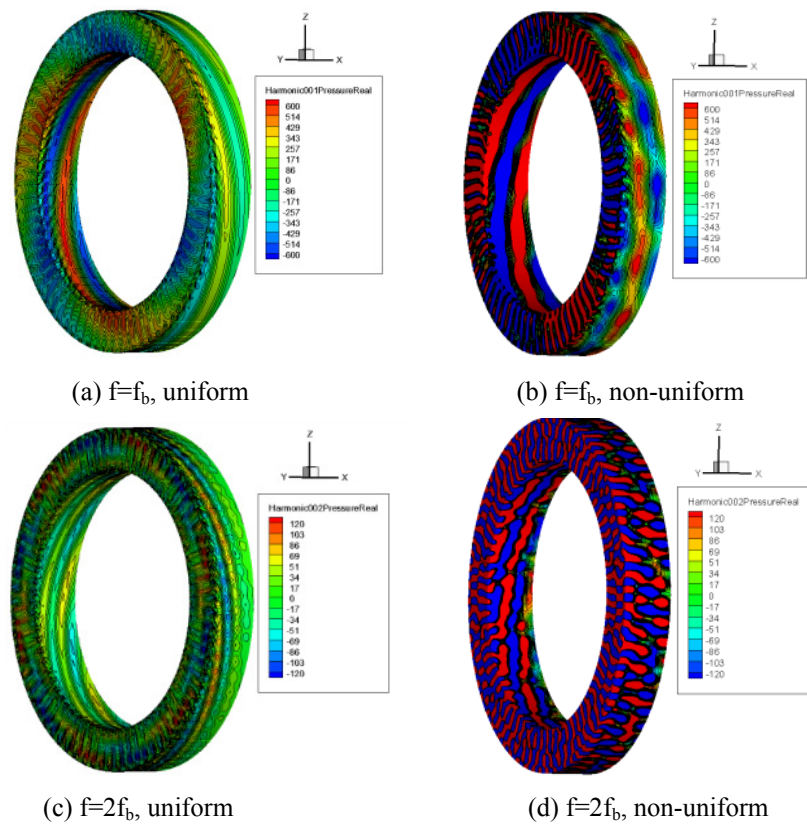
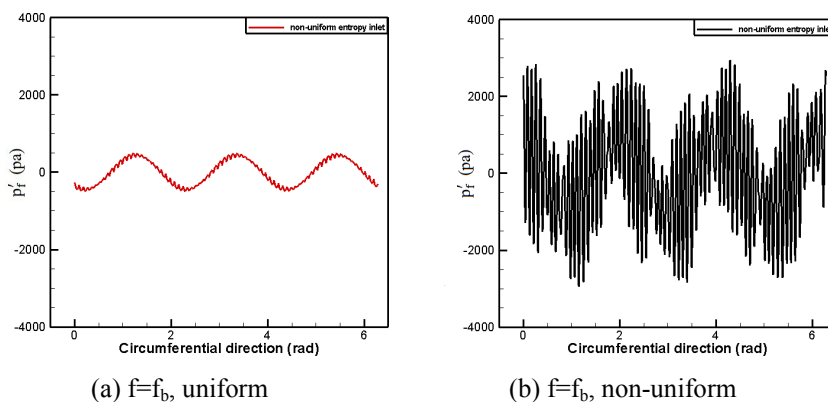


Figure 6. Distribution of fluctuation pressure on  $f_b$  and  $2f_b$



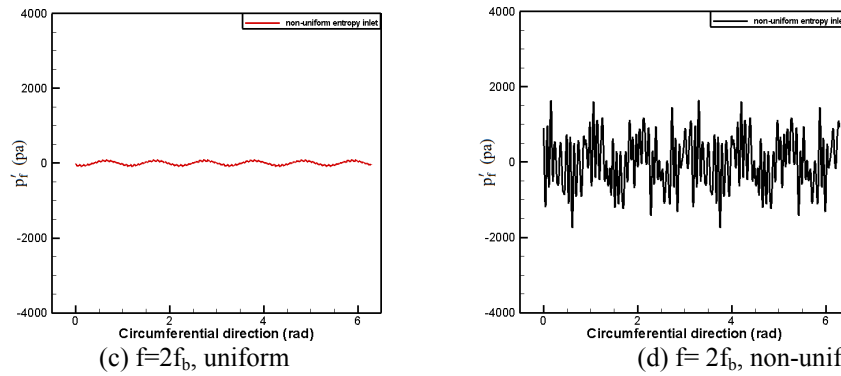


Figure 7. Distribution of fluctuation pressure on  $f_b$  and  $2f_b$  at  $x=0.148$  m in the mid-span radial position

### 3.3 Radial Mode Analysis

The comparison of Figure 6 and Figure 7 show the Fourier series expansion of the fluctuation pressure coefficients but not the sound field that propagates downstream. The pressure unsteadiness includes sound waves that are reflected from the downstream boundary and may contain pressure fluctuations due to cut-off modes. Part of the pressure field may also be connected to velocity fluctuation in the sheared flow near the casing or the hub and due to secondary flows downstream of the rotor. These fluctuations propagate with the flow speed and not the sound speed. The sound field shall be extracted now by using the Mode matching method which decomposes the fluctuation pressure field into acoustic radial duct modes. This allows to separate the downstream travelling modes from the upstream travelling modes.

In Figures 8, 9 and 10, the sound pressure level (SPL) of the cut-on modes with different radial modes in  $f=f_b$  and  $f=2f_b$  are shown. The modes  $m=3$ ,  $m=6$  and  $m=64$  are caused by both rotor-stator interaction and periodic total temperature-rotor interaction, while the other modes in Figure 9 and Figure 10 are only caused by periodic total temperature and rotor interaction. The difference of SPL between uniform and non-uniform case is almost 6 dB in  $(m, n) = (3, 1)$ , 11.54 dB in  $(m, n) = (6, 1)$ , and 28 dB in  $(m, n) = (-64, 1)$ . The sound pressure level in non-uniform case is increased obviously in all the radial modes.

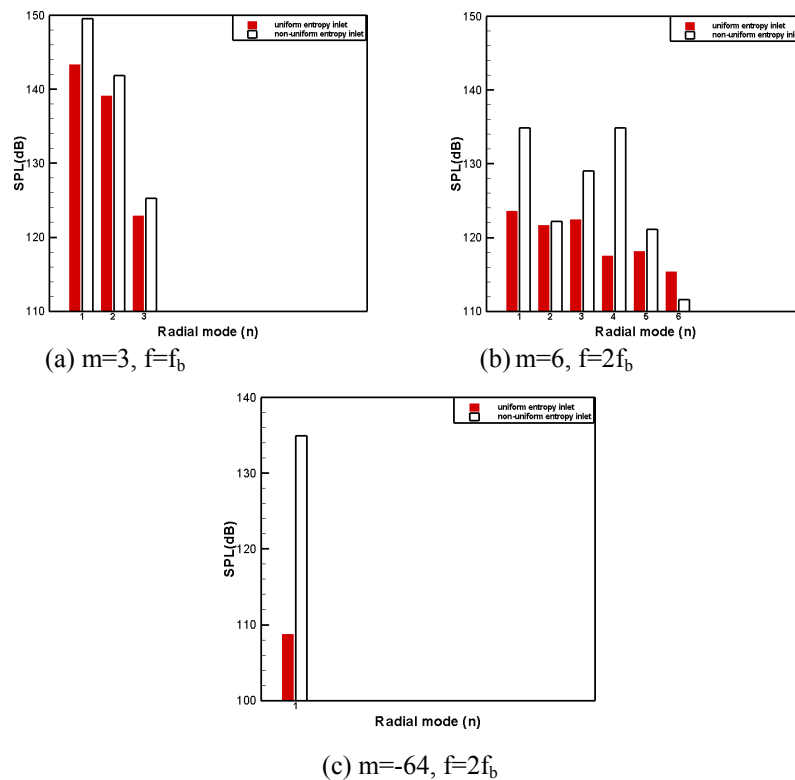


Figure 8. SPL of downstream travelling radial modes which caused by rotor-stator interaction and periodic total temperature-rotor interaction

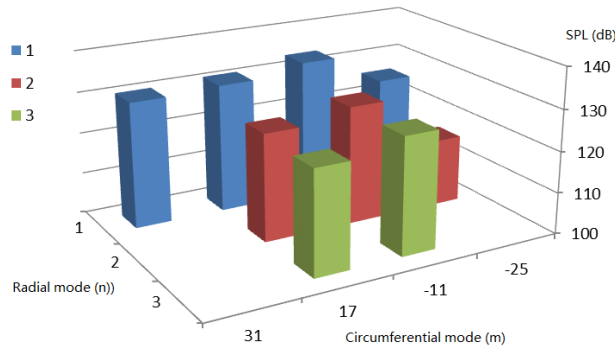


Figure 9. SPL of downstream travelling radial modes for  $f = f_b$  which caused by the periodic total temperature-rotor interaction

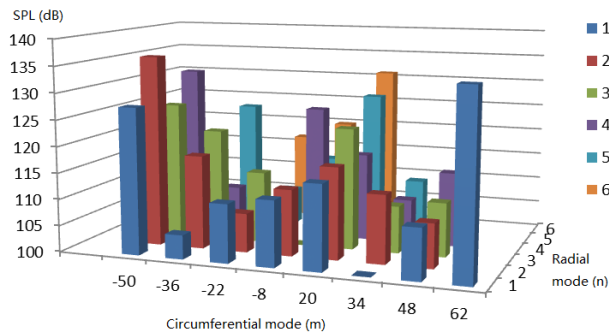


Figure 10. SPL of downstream travelling radial modes for  $f = 2f_b$  which caused by the periodic total temperature-rotor interaction

The amplitudes of radial modes show in Figures 8, 9 and 10 do not describe the acoustic power connected with it. The acoustic power can be estimated from the amplitudes (Holste, 1997). Figure 11 shows the acoustic power level on azimuthal modes for  $f_b$  and  $2f_b$ , The power of all radial modes are summed up for each  $m$ . The total acoustic power is also shown in Figure 11. The effect of non-uniform total temperature on the total acoustic power is about 5.93 dB for the blade-passing frequency and 11.66 dB for  $2f_b$ .

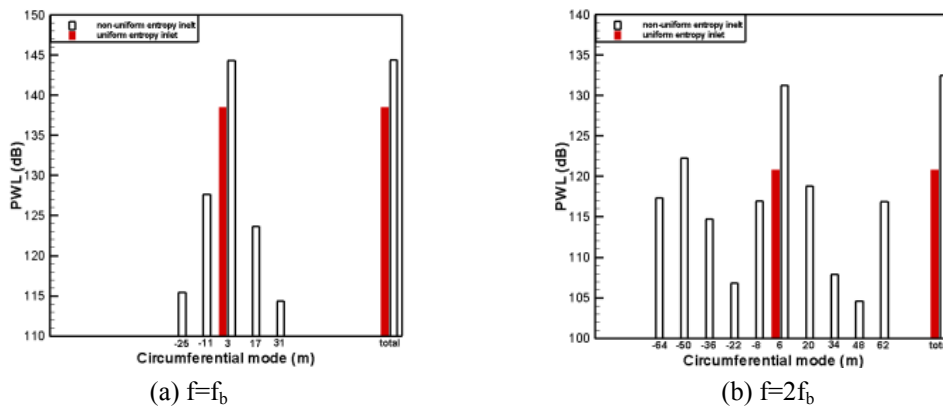


Figure 11. Acoustic power level (PWL) of downstream traveling

#### 4. Discussion

The sound emission of a high pressure turbine stage due to azimuthally periodic mean temperature distribution in the incoming flow is investigated numerically. We used 14 temperature periods with 70 stator passages and 73 rotor passages, which was more realistic compared to the case computed by Z. Mu. This present case has a wider periodic total temperature distribution. This improvement would make more circumferential modes cut on and to

make the interaction between periodic total temperature fluctuation and rotor stronger.

The tonal sound emission is studied downstream of the rotor for the blade passing frequency  $f_b$  and its first harmonic  $2f_b$ . The azimuthal mode has been divided into rotor stator interaction affecting modes and periodic total temperature rotor interaction affecting modes (Table 2). For the blade frequency, the dominance mode is  $m=3$ , and the modes  $m=-11$ ,  $m=17$ ,  $m=25$  and  $m=31$  are cut on. For the first harmonic of blade passing frequency, the dominance mode is  $m=6$ , and the modes  $m=-8$ ,  $m=20$ ,  $m=-22$ ,  $m=62$  and  $m=-64$  cut on.

The periodic total temperature-rotor interaction modes is because of the temperature fluctuation from the upstream inflow, in other words, the indirect combustion noise in a high pressure turbine stage is confirmed successfully. For the blade passing frequency, total acoustic power increased about 5.9 dB compared between uniform inlet temperature case and non-uniform inlet temperature case. For the second passing frequency, the total acoustic power increased dramatically about 11.66 dB. This result has shown that the temperature fluctuation because of the combustion would have a big affecting on the total sound power of a high pressure turbine stage.

## References

- Bake, F., Michel, U., & Rohle, I. (2007). Investigation of Temperature Noise in Aero-Engine Combustors. *J. Eng. Gas Turbines Power*, 129, 370-376. <http://dx.doi.org/10.1115/1.2364193>
- Bake, F., Kings, N., & Roehle, I. (2008). Fundamental Mechanism of Temperature Noise in Aero-Engines: Experimental Investigation. *J. Eng. Gas Turbines Power*, 130, 011202. <http://dx.doi.org/10.1115/1.2749286>
- Bake, F., & Richter, C. (2009). The Temperature Wave Generator (EWG): A reference case on temperature noise. *J. Sound Vib.*, 326, 574-598. <http://dx.doi.org/10.1016/j.jsv.2009.05.018>
- Cumpsty, N. A., & Marble, N. E. (1977). Core noise from gas-turbine exhausts. *J. Sound Vib.*, 54, 297-309. [http://dx.doi.org/10.1016/0022-460X\(77\)90031-1](http://dx.doi.org/10.1016/0022-460X(77)90031-1)
- Cumpsty, N. A. (1979). Jet engine combustion noise - Pressure, temperature and vorticity produced by unsteady combustion or heat addition. *J. Sound Vib.*, 66, 527-544. [http://dx.doi.org/10.1016/0022-460X\(79\)90697-7](http://dx.doi.org/10.1016/0022-460X(79)90697-7)
- He, L. (1992). Method of Simulating Unsteady Turbomachinery Flows with Multiple Perturbations. *AIAA Journal*, 30, 2730-2735. <http://dx.doi.org/10.2514/3.11291>
- Holste, F. (1997). An equivalent source method for calculation of the sound radiated from aircraft engines. *J. Sound Vib.*, 203(4), 667-695. <http://dx.doi.org/10.1006/jsvi.1996.0891>
- Kaplan, B., Nicke, E., & Voss, C. (2006). Design of a Highly Efficient Low-Noise Fan for Ultra High Bypass Engines. *ASME Turbo Expo 2006*, GT 2006-90363.
- Leykoa, M., Moreaud, S., & Poinso, T. (2009). Numerical and analytical investigation of the indirect combustion noise in a nozzle. *Combustion for aerospace propulsion, Comptes Rendus Mecanique*, 337, 415-425. <http://dx.doi.org/10.1016/j.crme.2009.06.025>
- Miles, J. (2010). Separating Direct and Indirect Turbofan Engine Combustion Noise Using the Correlation Function. *AIAA*, 2010-0019.
- Mu, Z., Michel, U., & Steger, M. (2010). Sound generation in a turbine stage due to non-uniform mean temperature flow. *AIAA*, 2010-397.
- Ovenden, N. C., & Rienstra, S. W. (2004). Mode matching Strategies in slowly varying Engine Ducts. *AIAA Journal*, 42, 1832-1840. <http://dx.doi.org/10.2514/1.3253>
- Tapken, U., Raitor, T., & Enghardt, L. (2009). Tonal Noise Reduction from an UHBR Fan - Optimized Inlet Radial Mode Analysis. *AIAA*, 2009-3288.
- Tyler, & Sofrin, T. G. (1962). Axial Flow Compressor Noise Studies. *Transactions of the Society of Automotive Engineers*, 70, 309-332.
- Zante, V. D., & Envia, E. (2009). Simulation of turbine tone noise generation using a turbomachinery aerodynamics solver. *AIAA*, 2009-3282.